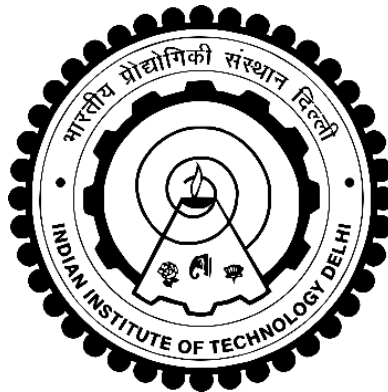


**SOME NOVEL APPLICATIONS OF DIGITAL  
SPECKLE PATTERN INTERFEROMETRY  
AND DIGITAL HOLOGRAPHIC  
INTERFEROMETRY**

**MANOJ KUMAR**



**INSTRUMENT DESIGN DEVELOPMENT CENTRE  
INDIAN INSTITUTE OF TECHNOLOGY DELHI  
HAUZ KHAS, NEW DELHI – 110016, INDIA**

**OCTOBER, 2016**

**© Indian Institute of Technology Delhi (IITD), New Delhi, 2016**

**SOME NOVEL APPLICATIONS OF DIGITAL  
SPECKLE PATTERN INTERFEROMETRY  
AND DIGITAL HOLOGRAPHIC  
INTERFEROMETRY**

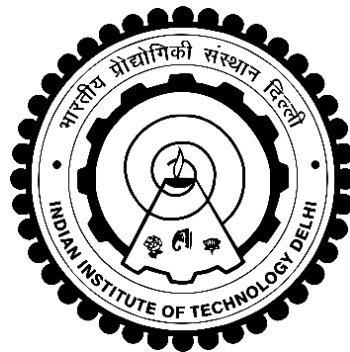
*by*

**MANOJ KUMAR**

**INSTRUMENT DESIGN DEVELOPMENT CENTRE**

*Submitted*

*in fulfilment of the requirements of the degree of Doctor of Philosophy  
to the*



**INDIAN INSTITUTE OF TECHNOLOGY DELHI**

**OCTOBER, 2016**

**DEDICATED**

**TO**

**MY FAMILY**

WHO ENCOURAGED AND SUPPORTED ME TO DO  
WHATEVER I WANTED TO DO, AND BE  
WHATEVER I WANTED TO BE

# CERTIFICATE

This is to certify that the thesis entitled “**SOME NOVEL APPLICATIONS OF DIGITAL SPECKLE PATTERN INTERFEROMETRY AND DIGITAL HOLOGRAPHIC INTERFEROMETRY**” being submitted by **Mr. MANOJ KUMAR** to the Indian Institute of Technology Delhi for the award of the degree of “**DOCTOR OF PHILOSOPHY**”, is a record of the authentic research work carried out by him under our supervision and guidance. He has fulfilled all the requirements for submission of this thesis, which to the best of my knowledge has reached the required standard.

The material contained in this thesis has not been submitted in part or full to any other University or Institute for the award of any other degree.

**Dr. Chandra Shakher**

Professor

Instrument Design Development Centre  
Indian Institute of Technology Delhi  
Hauz Khas – 110016  
New Delhi, India

**Dr. Gufran S. Khan**

Assistant Professor

Instrument Design Development Centre  
Indian Institute of Technology Delhi  
Hauz Khas – 110016  
New Delhi, India

# ACKNOWLEDGEMENTS

I owe thanks to several people who helped, supported and inspired me in many ways at different stages of my Ph.D. and made it an unforgettable experience for me.

First and the foremost, I would like to extend my special appreciation and sincere gratitude to my research supervisor **Prof. Chandra Shakher** who has introduced me to Speckle Metrology and Digital Holography – the intriguing field of science and engineering. The work reported in this thesis would not have been possible without his efficient and erudite guidance, continuous support, advice, inspiration, encouragement and motivation throughout my Ph.D. I successfully overcame many difficulties and learned this *beautiful field of metrology* under his guidance. His integral view on research and his mission for providing high-quality work has made a deep impression on me and I hope to continue to work with his noble thoughts. I also, express my profound indebtedness to him for the time he took out from his hectic schedule to guide me during the course of the thesis. He would have never accepted anything less than my best efforts, and for that, I thank him.

My special words of thanks should also go to my research supervisor **Dr. Gufran S. Khan**. His continuous support, guidance, cooperation, encouragement and motivation have always kept me going ahead. I owe a lot of gratitude to his scientific inputs, personal helps and friendly nature and I feel privileged to be associated with a person like him.

I am highly grateful to my Students Research Committee (SRC) members, **Prof. A.L. Vyas, Prof. M.R. Shenoy, and Prof. D.S. Mehta**, for their constructive comments and helpful suggestions during my progress report presentations.

A true friend is someone who reads the song in your heart and can sing it back to you, when you have forgotten the actual words. I have found such a friend in the form of **Ms. Shilpi Agarwal**. I cannot find the correct words to thank for her priceless and most prestigious support during my research work. She is my close friend and brilliant colleague who inspired me over the years. She was always there for me in my failures, weird situations and tolerated my frustrations and nonsenses but supported me throughout this period. I had shared many memorable moments and will always cherish these moments spent with her. I remember, knowingly or unknowingly I made her irritate many times but she never complained. Thank you for just being there when I need you.

I would like to express my deepest thanks and acknowledgements with gratitude and affection to fellow lab-mates **Dr. Gyanendra Sheoran, Dr. Shobhna Sharma, Mr. Varun Kumar, Ms. Sruthi Prasood, Ms. Monika, Mr. Avijit Prakash, and Mr. Pranav Kumar Pandey** for their support and co-operation as colleagues, who helped me in many ways at different stages of my thesis work in the Laser Applications and Holography Laboratory, IDD Centre, Indian Institute of Technology Delhi.

I appreciate and respect to **Dr. Vishal Srivastava** and **Dr. Mohd. Inam** for their moral support, valuable suggestions and sincere encouragement. I owe special thanks to **Dr. Vishal Srivastava** for discussions regarding image processing and other scientific issues.

I want to thank my special friends **Mr. Mahipal Bhumbla, Mr. Navdeep Phogat, Mr. Vikas Malik, Mr. Anil Malik, Mr. Sanjeet Kumar, and Mr. Anuj Prashar** with whom I spent very special time while playing, running, chatting, in any order and for all the fun we have had in the last few years during my stay in Shivalik Hostel. I cannot forget these friends because they went through my hard times with me, cheered me on and celebrated

each accomplishment. I am indebted to these friends for providing a stimulating and fun filled environment.

Words are short to express my deep sense of gratitude towards my following friends, **Ms. Ankita Gaur, Ms. Neelam Sehrawat, Mr. Tajber Singh, Mr. Rammurthy Godisela, Ms. Shweta Sehgal, Mr. Dinesh Bhardwaj, Mr. Asim Mahakula, Mr. Sharad Gupta, Mr. Yogesh Gupta, Mr. Naveen Bhardwaj, and Mr. Pankaj Mittal** with whom I shared my life experiences and they gave me reasons to go ahead with my work. These friends are used to talk regularly and help me to overcome the inevitable moments of demoralization.

Thanks are also to the technical staff of the workshop in Instrument Design Development Centre, IIT Delhi for the help rendered by them. I am thankful to **Mr. Surinder Singh and Mr. S.K. Bansal** for extending their valuable help at times.

The equipment used in the experiment which was purchased from Department of Science and Technology (**DST**), Govt. of India project is greatly acknowledged.

Last but not the least, I express deep sense of gratitude and loving thanks to **my parents** for their love, patience and inspiration in various stages of my research work and lifting me uphill this phase of life. I am grateful to my brother **Mr. Sundeep** and sister **Ms. Urmila** for their unending encouragement and helpful suggestions throughout this endeavor. Without their support and unconditional help, I would have never come so far.

Finally, I thank the almighty of God for giving me power to believe in myself and fulfil my dreams. There is no way to express how much it meant to me to have been a member of Laser Applications and Holography Laboratory.

Thank you all!

**Date:**

**Manoj Kumar**

# ABSTRACT

Optical interferometric techniques have proved enormous capabilities and potentials in scientific, engineering and industrial measurements. The interferometric techniques became more powerful and easy to implement after the invention of laser and holography. Holography and speckle interferometry added new dimensions in the interferometry by offering the capability to characterize rough mechanical surfaces with submicron accuracy and made it a powerful tool for the scientists and engineers to solve many problems of scientific and industrial importance. Further development in analog and digital electronics, electronic imaging devices, high speed digital computers and reliable image processing software has revolutionized optical measurement techniques. The optical interferometric techniques have become automated, effective, and easier to visualize the measurement results.

Digital speckle pattern interferometry (DSPI) and digital holographic interferometry (DHI) are widely used promising evaluation optical measurement techniques. Both these techniques are developed independently but can be regarded as two experimental approaches of the same concept of interferometry for transparent, opaque and diffusely scattering objects. The goal of this thesis is to design and develop the DSPI and DHI systems for investigating the various scientific and industrial measurements.

The thesis is divided into six chapters:

**Chapter 1** outlines the detailed description of DSPI and DHI and their applications in metrology. A review of phase extraction techniques and proposed phase extraction method, i.e. Riesz transform and monogenic signal, is described in detail. A brief description of

digital holography including the numerical reconstruction of digitally recorded holograms is provided in the next section. A brief outline of the research contribution and scope of this research work is presented at the end of the chapter.

**Chapter 2** provides the application of DSPI for the measurement of temperature and evaluation of temperature profile of diffusion, premixed and partially premixed flames obtained from butane torch burner under the influence of uniform magnetic field, upward-decreasing magnetic gradient field and upward-increasing magnetic gradient field.

**Chapter 3** demonstrates the use of digital speckle pattern shearing interferometry (DSPSI) where the shear is created by volume phase holographic grating to measure the temperature and temperature profile of diffusion flame (candle flame). The proposed DSPSI system is simple, compact, requires low mechanical stability and less vibration sensitive.

**Chapter 4** describes an application of DSPI for the measurement of deformations and strain-field distributions developed in cortical bone around orthodontic miniscrew implants of different diameters and lengths inserted into the human maxilla is presented.

**Chapter 5** demonstrates the application of Lensless Fourier transform digital holographic interferometry (LLFTDHI) to study the effect of moisture on the dimensional changes of different samples of wood. Further, investigations are done to determine the induced strain due to the shrinkage of wood and to measure the hygroscopic shrinkage coefficients during the convective drying process of differently treated seasoned woods.

**Chapter 6** summarizes the main points of research work and also some potential further development scopes related to our findings in optical metrology.

# CONTENTS

<b>CERTIFICATE</b>	<b>i</b>
<b>ACKNOWLEDGEMENTS</b>	<b>ii</b>
<b>ABSTRACT</b>	<b>v</b>
<b>CONTENTS</b>	<b>x</b>
<b>LIST OF FIGURES</b>	<b>xv</b>
<b>LIST OF TABLES</b>	<b>xxiii</b>
<b>LIST OF ABBREVIATIONS</b>	<b>xxiv</b>
<b>LIST OF SYMBOLS</b>	<b>xvii</b>
<b>CHAPTER 1: DIGITAL SPECKLE PATTERN</b>	
<b>INTERFEROMETRY AND DIGITAL</b>	<b>1-56</b>
<b>HOLOGRAPHIC INTERFEROMETRY</b>	
1.1 Introduction.....	1
1.2 Historical Background of Speckle Effect.....	2
1.3 Speckle Effect.....	5
1.4 Properties of Speckle.....	8
1.4.1 Statistical Intensity Distribution.....	8
1.4.2 Contrast of Speckle Pattern.....	10
1.5 Speckle Metrology.....	10
1.5.1 Speckle Photography.....	11

1.5.2 Speckle Interferometry.....	12
1.5.3 Electronic Speckle Pattern Interferometry (ESPI) and Digital Speckle Pattern Interferometry (DSPI).....	18
1.5.4 Processing of Specklegrams in DSPI.....	23
1.5.5 Speckle Shear Interferometry.....	26
1.6 Phase Extraction from a Single DSPI Fringe Pattern.....	29
1.6.1 Phase Extraction Techniques in Interferometry.....	29
1.6.2 Riesz Transform and Monogenic Signal.....	35
1.7 Digital Holography.....	39
1.8 Recording of Digital Holograms.....	40
1.9 Numerical Reconstruction of Holograms.....	43
1.9.1 Finite Discrete Fresnel Transform.....	46
1.9.2 Lensless Fourier Transform.....	49
1.10 Digital Holographic Interferometry and its Applications.....	54
1.11 Outline of Research Work Done in this Thesis.....	56

**CHAPTER 2: MEASUREMENT OF TEMPERATURE AND  
TEMPERATURE PROFILE OF AXI-  
SYMMETRIC BUTANE FLAMES UNDER THE  
EFFECT OF MAGNETIC FIELD BY USING  
DIGITAL SPECKLE PATTERN  
INTERFEROMETRY** 57-82

2.1 Introduction.....	57
-----------------------	----

2.2 Theory.....	61
2.3 Experimental.....	66
2.4 Results.....	70
2.4.1 In the Absence of Magnetic Field.....	70
2.4.2 Uniform Magnetic Field.....	73
2.4.3 Upward-decreasing Magnetic Field.....	73
2.4.4 Upward-increasing Magnetic Field.....	74
2.5 Discussion.....	76
2.6 Characterization of Diffusion Flame of Butane under Magnetic Gradient.....	78
2.6.1 Magnetic Grashof Number.....	78
2.6.2 Reynolds Number.....	79
2.6.3 Magnetic Froude Number.....	80
2.7 Conclusion.....	81

**CHAPTER 3: MEASUREMENT OF TEMPERATURE AND  
TEMPERATURE DISTRIBUTION IN GASEOUS  
FLAMES BY DIGITAL SPECKLE PATTERN  
SHEARING INTERFEROMETRY USING  
HOLOGRAPHIC OPTICAL ELEMENT** **83-96**

3.1 Introduction .....	83
3.2 Theory.....	85
3.3 Experimental.....	88

3.4 Results and Discussion.....	92
3.5 Conclusion.....	96

**CHAPTER 4: MEASUREMENT OF STRAIN DISTRIBUTION  
AROUND MINISCREW IMPLANTS USED FOR  
ORTHODONTIC ANCHORAGE USING  
DIGITAL SPECKLE PATTERN  
INTERFEROMETRY** **97-116**

4.1 Introduction.....	97
4.3 Theory.....	101
4.3.1 Determination of Surface Deformations and Strains.....	102
4.3.2 Determination of Tilt Rotation of Canine.....	103
4.4 Experimental.....	104
4.5 Results .....	109
4.6 Discussion.....	114
4.7 Conclusion.....	116

**CHAPTER 5: CHARACTERIZATION OF HYGROSCOPIC  
PROPERTIES OF WOODS DURING  
CONVECTIVE DRYING USING DIGITAL  
HOLOGRAPHIC INTERFEROMETRY** **117-140**

5.1 Introduction .....	117
5.2 Theory.....	120
5.2.1 Recording and Numerical Reconstruction of Digital Holograms.....	120



# LIST OF FIGURES

Figure No.	Figure Caption	Page No.
<b>Fig. 1.1(a)</b>	Objective speckle pattern.....	6
<b>Fig. 1.1(b)</b>	Subjective speckle pattern.....	6
<b>Fig. 1.2</b>	Probability density function taken from a speckle pattern.....	9
<b>Fig. 1.3</b>	Geometric relation of the light source, image plane and the object...	15
<b>Fig. 1.4(a)</b>	Optical arrangements for measurement of out-of-plane displacement.....	16
<b>Fig. 1.4(b)</b>	Optical arrangements for measurement of in-plane displacement....	17
<b>Fig. 1.5</b>	Typical experimental arrangement of ESPI.....	19
<b>Fig. 1.6</b>	Block diagram of DSPI system including the speckle interferometer and the digital electronics part.....	22
<b>Fig. 1.7</b>	Michelson interferometer based speckle shear interferometer.....	28
<b>Fig. 1.8</b>	Phase shifting by linear displacement of reference surface using PZT.....	30
<b>Fig. 1.9</b>	Angular extent of object.....	42
<b>Fig. 1.10</b>	Schematic of recording of off-axis digital hologram.....	43
<b>Fig. 1.11</b>	Schematic of Cartesian coordinate system used for recording and reconstruction of digital holography.....	44
<b>Fig. 1.12</b>	Schematic of recording of lensless Fourier hologram.....	49
<b>Fig. 1.13(a)</b>	Geometry showing the variation of angle between object wave and plane reference wave over the detector surface.....	50
<b>Fig. 1.13(b)</b>	Geometry showing the variation of angle between object and spherical reference wave over the detector surface.....	50
<b>Fig. 1.14</b>	Schematic of experimental setup for LLFTDH.....	52

<b>Fig. 1.15</b>	Process for the reconstruction of digital hologram.....	53
<b>Fig. 1.16(a)</b>	Real image, virtual image and DC term of a screw reconstructed using LLFTDH.....	54
<b>Fig. 1.16(b)</b>	Real image after removing of virtual image and dc term.....	54
<b>Fig. 1.17</b>	Optical path length difference between two different object states...	55
<b>Fig. 2.1(a)</b>	DSPI system for the measurement out-of-plane displacement.....	63
<b>Fig. 2.1(b)</b>	DSPI fringe pattern for 2 $\mu$ m displacement.....	63
<b>Fig. 2.1(c)</b>	DSPI fringe pattern for 4 $\mu$ m displacement.....	63
<b>Fig. 2.1(d)</b>	DSPI fringe pattern for 8 $\mu$ m displacement.....	63
<b>Fig. 2.1(e)</b>	Riesz transform components along $x$ -axis.....	64
<b>Fig. 2.1(f)</b>	Riesz transform components along $y$ -axis.....	64
<b>Fig. 2.1(g)</b>	Wrapped phase difference map 2 $\mu$ m displacement corresponding to Fig. 2.1(b).....	64
<b>Fig. 2.2(a)</b>	Schematic of DSPI setup for measurement of temperature in the presence of magnetic field.....	67
<b>Fig. 2.2(b)</b>	Photograph of the experimental setup for measurement of temperature in the presence of magnetic field.....	68
<b>Fig. 2.3</b>	Schematic representation of different positions of flame in magnetic gradient field.....	69
<b>Fig. 2.4(a)</b>	DSPI fringe pattern of diffusion flame of butane torch burner in the absence of magnetic field.....	69
<b>Fig. 2.4(b)</b>	DSPI fringe pattern of diffusion flame of butane torch burner in the presence of uniform magnetic field.....	69
<b>Fig. 2.4(c)</b>	DSPI fringe pattern of diffusion flame of butane torch burner in the presence of upward-decreasing magnetic field.....	69
<b>Fig. 2.4(d)</b>	DSPI fringe pattern of diffusion flame of butane torch burner in the presence of upward-increasing magnetic field.....	69

<b>Fig. 2.5</b>	Flow chart of the experimental and process for calculation of refractive index change and temperature profile.....	70
<b>Fig. 2.6(a)</b>	Riesz components of diffusion flame corresponding to Fig. 2.4(a) on $x$ -axis.....	71
<b>Fig. 2.6(b)</b>	Riesz components of diffusion flame corresponding to Fig. 2.4(a) on $y$ -axis.....	71
<b>Fig. 2.6(c)</b>	The retrieved wrapped phase of diffusion flame in the absence of magnetic field corresponding to Fig. 2.4(a).....	71
<b>Fig. 2.6(d)</b>	The plot of unwrapped phase of half width of diffusion flame in the absence of magnetic field along the line AB. A smoothing spline interpolation has been used for the curve fitting.....	71
<b>Fig. 2.6(e)</b>	Refractive index profile along the line AB corresponding to Fig. 2.6(c).....	71
<b>Fig. 2.6(f)</b>	The temperature distribution of the diffusion flame in the absence of magnetic field corresponding to Fig. 2.6(c) along the line AB...	72
<b>Fig. 2.7(a)</b>	Wrapped phase of diffusion flame in the presence of uniform magnetic field corresponding to Fig. 2.4(b).....	73
<b>Fig. 2.7(b)</b>	Temperature distribution of diffusion flame in the presence of uniform magnetic field corresponding to Fig. 2.7(a) along the line AB.....	73
<b>Fig. 2.8(a)</b>	Wrapped phase of diffusion flame in the presence of upward-decreasing magnetic field corresponding to Fig. 2.4(c).....	74
<b>Fig. 2.8(b)</b>	The temperature distribution of diffusion flame in the presence of upward-decreasing magnetic field corresponding to Fig. 2.8(a) along the line AB.....	74
<b>Fig. 2.9(a)</b>	Wrapped phase of diffusion flame in the presence of upward-increasing magnetic field corresponding to Fig. 2.4(d).....	75

<b>Fig. 2.9(b)</b>	The temperature distribution of diffusion flame in the presence of upward-increasing magnetic field corresponding to Fig. 2.9(a) along the line AB.....	75
<b>Fig. 2.10</b>	Flow of paramagnetic and diamagnetic gases in upward-decreasing magnetic gradient field.....	77
<b>Fig. 2.11(a)</b>	The plot of magnetic field distribution in upward-decreasing magnetic field configuration.....	79
<b>Fig. 2.11(b)</b>	The plot of magnetic field distribution in upward-increasing magnetic field configuration.....	79
<b>Fig. 2.12</b>	Recorded interferograms showing the change in flame size.....	81
<b>Fig. 3.1</b>	Light ray crossing the radially symmetric flame.....	86
<b>Fig. 3.2(a)</b>	Schematic of DSPSI setup for measurement of temperature in gaseous flames.....	89
<b>Fig. 3.2(b)</b>	Photograph of the DSPSI setup for measurement of temperature in gaseous flames.....	89
<b>Fig. 3.3</b>	Mechanism of the wavefront shearing using volume phase holographic grating and ground glass.....	91
<b>Fig. 3.4</b>	DSPSI fringe pattern of candle flame.....	91
<b>Fig. 3.5</b>	Flow chart of the experimental and process for calculation of refractive index change and temperature profile.....	92
<b>Fig. 3.6(a)</b>	Riesz components of candle flame corresponding to Fig. 3.4 on $x$ -axis.....	93
<b>Fig. 3.6(b)</b>	Riesz components of candle flame corresponding to Fig. 3.4 on $y$ -axis.....	93
<b>Fig. 3.6(c)</b>	The retrieved wrapped phase of candle flame corresponding to Fig. 3.4.....	93

<b>Fig. 3.7(a)</b>	The plot of unwrapped phase of half width of the candle flame along the line AB. A smoothing spline interpolation has been used for the curve fitting.....	95
<b>Fig. 3.7(b)</b>	Refractive index profile along the line AB corresponding to Fig. 3.6(c).....	95
<b>Fig. 3.8</b>	The temperature distribution of the candle flame corresponding to Fig. 3.6(c) along the line AB.....	95
<b>Fig. 4.1(a)</b>	Miniscrew implants.....	105
<b>Fig. 4.1(b)</b>	Implant drivers.....	105
<b>Fig. 4.2</b>	Human skull with complete strap up in maxillary arch with inserted miniscrew implant.....	105
<b>Fig. 4.3</b>	Photograph of the human maxilla used in the experiment with nickel-titanium coil spring attached to the head of miniscrew implant and to the hook of canine bracket for implant loading.....	106
<b>Fig. 4.4(a)</b>	Schematic of DSPI set-up for measurement of out-of-plane and in-plane deformation and strain in human maxilla.....	107
<b>Fig. 4.4(b)</b>	Photograph of DSPI setup for measurement of out-of-plane and in-plane deformation in human maxilla.....	108
<b>Fig. 4.5(a)</b>	DSPI fringe pattern of out-of-plane deformation.....	108
<b>Fig. 4.5(b)</b>	DSPI fringe pattern of in-plane deformation.....	108
<b>Fig. 4.6</b>	Flow chart of the experimental and process for calculation of strain in human maxilla.....	109
<b>Fig. 4.7</b>	Process of calculating phase extraction and out-of-plane displacement/deformation in cortical bone around miniscrew implant from DSPI fringe pattern by using Riesz transform method.	110

<b>Fig. 4.8</b>	Surface displacement in cortical bone around miniscrew implants of Bio-material of different lengths (L) and diameters (D) - (a) L=6mm, D=1.2 mm, (b) L=7 mm, D=1.2 mm, (c) L=6 mm, D=1.5mm and (d) L=7 mm, D=1.5 mm.....	111
<b>Fig. 4.9</b>	Surface displacement in cortical bone around miniscrew implants of Dentos of different lengths (L) and diameters (D) - (a) L= 6mm, D=1.2 mm, (b) L=7 mm, D=1.2 mm, (c) L=6 mm, D=1.5 mm and (d) L=7 mm, D=1.5 mm.....	112
<b>Fig. 4.10</b>	Process of phase extraction and displacement measurement in canine from recorded DSPI fringe pattern by using Riesz transform.	113
<b>Fig. 5.1(a)</b>	Schematic of the experimental setup used for the recording of digital holograms.....	125
<b>Fig. 5.1(b)</b>	Photograph of the experimental setup used for the recording of digital holograms.....	125
<b>Fig. 5.2(a)</b>	Schematic of total cumulative shrinkage in tangential, radial and longitudinal directions.....	126
<b>Fig. 5.2(b)</b>	Photograph of the devadar wood used in the experiment.....	127
<b>Fig. 5.2(c)</b>	Photograph of marandi wood used in the experiment.....	127
<b>Fig. 5.2(d)</b>	Photograph of plywood used in the experiment.....	127
<b>Fig. 5.3(a)</b>	Reconstructed phase difference map of devadar wood corresponding to moisture step change of 42.9% to 40.57% (SI/SNR=0.5940/1.6835).....	127
<b>Fig. 5.3(b)</b>	Phase difference map after implementation of median filter (3×3) (SI/SNR=0.2214/4.5174).....	127
<b>Fig. 5.3(c)</b>	Phase difference map after implementation of windowed Fourier filtering (SI/SNR=0.0587/17.0425).....	127
<b>Fig. 5.4</b>	Unwrapped phase difference map corresponding to Fig. 5.3(c).....	128

<b>Fig. 5.5</b>	Unwrapped phase difference maps of devadar wood at different moisture contents (MC) recorded at an interval of 20 minutes during convective drying.....	129-130
<b>Fig. 5.6</b>	Displacement map resulting from the reference hologram (recorded at 42.90% moisture content) and the hologram recorded after 20 minutes (at 40.57% moisture content) corresponding to Fig. 5.4(c)..	131
<b>Fig. 5.7</b>	The derivative of out-of-plane deformation resulting from the reference hologram (recorded at 42.90% MC) and the hologram recorded after 20 minutes (at 40.57% MC) corresponding to displacement map shown in Fig. 5.6.....	132
<b>Fig. 5.8</b>	Hygroscopic shrinkage strain behaviour of devadar wood as a function of moisture content.....	132
<b>Fig. 5.9</b>	Hygroscopic shrinkage strain behaviour of devadar wood with time	133
<b>Fig. 5.10</b>	Hygroscopic shrinkage strain behaviour as a function of moisture content for devadar wood at three different seasoning cases.....	134
<b>Fig. 5.11</b>	Hygroscopic shrinkage coefficient as function of moisture content for devadar wood at three different conditioning cases.....	135
<b>Fig. 5.12</b>	Hygroscopic shrinkage strain behaviour as a function of moisture content for <i>marandi</i> wood at three different conditioning cases.....	136
<b>Fig. 5.13</b>	Hygroscopic shrinkage coefficient as function of moisture content for <i>marandi</i> wood at three different conditioning cases. The variation in hygroscopic shrinkage coefficient is almost constant for the case of properly conditioned wood (shown by blue line).....	136
<b>Fig. 5.14</b>	Hygroscopic shrinkage strain behaviour as a function of moisture content for plywood at three different conditioning cases.....	137
<b>Fig. 5.15</b>	Hygroscopic shrinkage coefficient as function of moisture content for plywood at three different seasoning cases.....	138

# LIST OF TABLES

<b>Table No.</b>	<b>Table caption</b>	<b>Page No.</b>
<b>Table 2.1</b>	Maximum temperature for butane torch burner flames in various magnetic field configurations.....	75
<b>Table 2.2</b>	Parameters used in the experiment.....	80
<b>Table 4.1</b>	Geometric parameters of investigating miniscrew implants.....	104
<b>Table 4.2</b>	Elastic material properties of variables used.....	105
<b>Table 4.3</b>	Calculated values of displacement and tilt rotation in canine.....	113
<b>Table 4.4</b>	Calculated values of displacement and strain in cortical bone around miniscrew implant.....	114
<b>Table 5.1</b>	Percentage decrease of hygroscopic shrinkage strain for devadar wood.....	138
<b>Table 5.2</b>	Percentage decrease of hygroscopic shrinkage strain for marandi wood.....	138
<b>Table 5.3</b>	Percentage decrease of hygroscopic shrinkage strain for plywood.....	139

# LIST OF ABBREVIATIONS

<b>Abbreviation</b>	<b>Definition</b>
DSPI	Digital speckle pattern interferometry
DHI	Digital holographic interferometry
DH	Digital holography
LLFTDH	Lensless Fourier transform digital holography
LLFTDHI	Lensless Fourier transform digital holographic interferometry
ESPI	Electronic speckle pattern interferometry
A/D	Analog-to-digital
CCD	Charge-couple device
CMOS	Complementary metal-oxide semiconductor
HOE	Holographic optical element
FFT	Fast Fourier transform
IFFT	Inverse fast Fourier transform
SPS	Spatial phase-shifting
TPS	Temporal phase-shifting
PZT	Piezoelectric transducer
FTM	Fourier transform method
CWT	Continuous Wavelet transform
HT	Hilbert transform
EMD	Empirical mode decomposition
SNR	Signal-to-noise ratio
<i>Re</i>	Real function
<i>Im</i>	Imaginary function
DSPSI	Digital speckle pattern shearing interferometer

FEM	Finite element method
CT	Computed tomography
DIC	Digital image correlation
WFT	Windowed Fourier transform
WFF	Windowed Fourier filtering
MC	Moisture content

# LIST OF SYMBOLS

$\sigma_o$	Average diameter of objective speckle
$\sigma_s$	Average diameter of subjective speckle
$d_o$	Average diameter of a circular illuminated patch of the diffused object
$d$	Distance between object and image plane
$\lambda$	Wavelength of laser light used
$F$	$f$ -number of the imaging lens
$M$	Magnification of the imaging lens
$A(x, y, z)$	complex amplitude of the object wave at the point $O(x,y,z)$
$a_n$	Amplitude of the $n^{\text{th}}$ scattered elementary wave
$\phi_n$	Phase of the $n^{\text{th}}$ scattered elementary wave
$p(I)$	Probability distribution of speckle pattern
$I$	Intensity of the speckle pattern
$\langle I \rangle$	Average intensity of the speckle pattern
$\sigma$	Standard deviation of speckle pattern
$\gamma$	Normalized standard deviation of speckle pattern, or speckle index
$a_o$	Amplitude of the object wave
$\phi_o$	Phase of the object wave
$a_r$	Amplitude of the reference wave
$\phi_r$	Phase of the object reference wave
$I_o$	Intensities of the object wave
$I_r$	Intensities of the reference wave

$\phi = (\phi_o - \phi_r)$	Random phase of the speckle interferogram
$\Delta\Phi$	Additional phase difference introduced by either object deformation or by refractive index fluctuation
$I(x, y)$	Resultant intensity distribution of two speckle interferograms,
$k_1$	Propagation vector of illumination beam
$k_2$	Propagation vector of observation beam
$k_s$	Sensitivity vector
$d_x, d_y, d_z$	Deformation vector of a point $O(x, y)$ on the object surface along $x$ -, $y$ -, $z$ -directions respectively
$e_x, e_y, e_z$	Unit vectors in $x, y, z$ - directions respectively
$\theta_{xz}$	Angle between the illumination and observation vectors in the $x, z$ -plane
$\psi_0$	Phase of vibration of the object
$\omega$	Angular frequency of vibration
$J_0$	Zeroth-order Bessel function
$a$	Amplitude of vibration
$\Delta x$	Lateral shear in $x$ -direction
$\gamma_0$	Amplitude modulation term
$\alpha_i$	Average value of relative phase shift for $i^{\text{th}}$ exposure
$\xi$	Spatial frequency along $x$ -direction
$\xi_0$	Spatial carrier
$I(\xi, y)$	Fourier transform of $I_0(x, y)$
$C(\xi - \xi_0, y)$	Fourier transform of $c(x, y) \exp(i2\pi\xi_0 x)$
$C^*(\xi - \xi_0, y)$	Fourier transform of $c^*(x, y) \exp(-i2\pi\xi_0 x)$

$W(b', a, \theta)$	Wavelet transform coefficient
$\psi(X)$	Mother wavelet
$R[.]$	Riesz operator
$\hat{H}(k)$	Transfer function of the Riesz transform
$I_x(x, y)$	Riesz transform components on $x$ - axis
$I_y(x, y)$	Riesz transform components on $y$ - axis
$R_x$	Spatial representation of the Riesz kernel on $x$ - axis
$R_y$	Spatial representation of the Riesz kernel on $y$ - axis
$S_M(x, y)$	3-D monogenic signal
$\vartheta$	Orientation between two Riesz transform components
$f_{\max}$	Maximum spatial frequency of the CCD/CMOS detector
$Q$	Fringe spacing
$\theta_{\max}$	Maximum angle between the object and the reference beams
$\Delta X$	Pitch of the CCD/CMOS detector
$X_0$	X coordinate in object plane
$Y_0$	Y coordinate in object plane
$X_H$	X coordinate in hologram plane
$Y_H$	Y coordinate in hologram plane
$X_I$	X coordinate in image plane
$Y_I$	Y coordinate in image plane
$O$	Complex amplitude of the object wave
$O^*$	Complex conjugate of the object wave
$R$	Complex amplitude of the reference wave
$R^*$	Complex conjugate of the reference wave
$I(X_H, Y_H)$	Intensity distribution of the interference pattern at hologram plane

$I(p, q)$	Digital hologram
$\Delta X_H$	Sampling interval along X-axis in hologram plane
$\Delta Y_H$	Sampling interval along Y-axis in hologram plane
$\Delta X_I$	Sampling interval along X-axis in image plane
$\Delta Y_I$	Sampling interval along Y-axis in image plane
$L \times B$	Dimensions of CCD/CMOS detector
$M \times N$	Number of pixels in CCD/CMOS detector
$O(X_I, Y_I)$	Complex amplitude of reconstructed object wave in image plane
$\rho'$	Distance between a point in hologram plane and a point in the image plane
$R(p, q)$	Digitized reference wave
$\phi(m, n)$	Phase distribution of reconstructed object wavefield
$\Delta\Phi(m, n)$	Phase difference of reconstructed object wavefields
$n(r)$	Refractive index of the medium
$n_o$	Refractive index of the air (reference state)
$T$	Temperature to be calculated
$T_0$	Temperature at the reference condition (Room temperature)
$P$	Atmospheric pressure
$R$	Universal gas constant
$A$	Molar refractivity of air at 632.8 nm ( $4.606 \times 10^{-6} \text{ m}^3/\text{mol}$ )
$\chi$	Magnetic susceptibility (subscripts $f$ for fuel and $ox$ for oxygen)
$F_{mag}$	Magnetic body force
$B$	Magnetic induction (Tesla)
$\frac{dB}{dz}$	Magnetic gradient field in z-direction
$\mu_0$	Magnetic permeability of free space (Henry per meter)

$Gr_m$	Magnetic Grashoff number
$Fr_m$	Magnetic Froude number
$Re$	Reynolds number
$\rho$	Density of fuel (butane) (Kg/m <sup>3</sup> )
$\nu$	Viscosity of the fuel (N-s/m <sup>2</sup> )
$u$	Fuel velocity (m/s)
$b$	Diameter of burner tube (m)
$l'$	Distance between magnetic poles (m)
$s$	Amount of shear
$\alpha$	Angle of incident light on the volume phase holographic grating
$\beta$	Angle in which the first order is diffracted
$\varepsilon$	Strain
$f$	Focal length of the imaging lens